Enhanced Lifetime of Polymer Solar Cells by Surface Passivation of Metal Oxide Buffer Layers

Swaminathan Venkatesan,[†,‡,§] Evan Ngo,[†,‡] Devendra Khatiwada,[‡] Cheng Zhang,[§] and Qiquan Qiao*[,‡]

[‡]Center for Advanced Photovoltaics, Department of Electrical Engineering and Computer Science, and [§]Department of Chemistry and Biochemistry, South Dakota State University, Brookings, South Dakota 57006, United States

S Supporting Information

ABSTRACT: The role of electron selective interfaces on the performance and lifetime of polymer solar cells were compared and analyzed. Bilayer interfaces consisting of metal oxide films with cationic polymer modification namely poly ethylenimine ethoxylated (PEIE) were found to enhance device lifetime compared to bare metal oxide films when used as an electron selective cathode interface. Devices utilizing surface-modified metal oxide layers showed enhanced lifetimes, retaining up to 85% of their original efficiency when stored in ambient atmosphere for 180 days without any encapsulation. The work function and surface potential of zinc oxide (ZnO) and ZnO/PEIE interlayers were evaluated using Kelvin probe and Kelvin probe force microscopy (KPFM) respectively. Kelvin probe measurements showed a smaller reduction in work function of ZnO/PEIE films compared to bare ZnO films when aged in atmospheric conditions. KPFM measurements showed that the surface potential of the ZnO surface drastically reduces when stored in ambient air for 7 days because of surface oxidation. Surface oxidation of the interface led to a substantial decrease in the performance in aged devices. The enhancement in the lifetime of devices with a bilayer interface was correlated to the suppressed surface oxidation of the metal oxide layers. The PEIE passivated surface retained a lower Fermi level when aged, which led to lower trap-assisted recombination at the polymer–cathode interface. Further photocharge extraction by linearly increasing voltage (Photo-CELIV) measurements were performed on fresh and aged samples to evaluate the field required to extract maximum charges. Fresh devices with a bare ZnO cathode interlayer required a lower field than devices with ZnO/PEIE cathode interface. However, aged devices with ZnO required a much higher field to extract charges while aged devices with ZnO/PEIE showed a minor increase compared to the fresh devices. Results indicate that surface modification can act as a suitable passivation layer to suppress oxidation in metal oxide thin films for enhanced lifetime in inverted organic solar cells.

KEYWORDS: polymer solar cells, surface passivation, metal oxide, and buffer layer
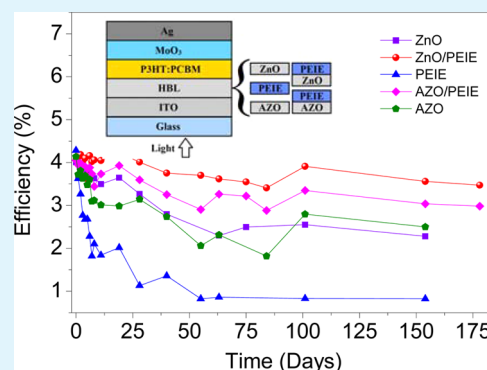
INTRODUCTION

Organic photovoltaics have become a strong focus of study because of the inherent flexibility and ability for mass production without requiring vacuum processing.[1,2] There are also a large range of film deposition techniques that can be applied to manufacturing organic photovoltaic devices, further increasing the versatility of the technology.[3–5] The primary factors limiting large-scale production of organic photovoltaic devices include the efficiency and lifetime, both of which are lower than inorganic-based solar cells. In the case of polymer cells, degradation predominantly occurs due to exposure to atmospheric oxygen or water, ultraviolet light and when subjected to higher temperatures.[6–8] Conventional organic solar cells employ PEDOT:PSS as hole transport layer and low work function metals such as calcium and aluminum as cathodes. These cells show reduced lifetime due to use of low work function metal cathodes that oxidize in air and also due to the acidic and hygroscopic nature of PEDOT:PSS.[9,10] Inverted solar cells, which consist of a transparent electrode as a cathode and high work function metal films as an anode have shown

higher device performance and longer lifetime due to preferred vertical phase segregation in the active layer and improved stability of metal anodes, respectively.[11,12] In inverted devices, metal oxide layers such as zinc oxide,[13] titanium oxide[14] and other transition metal oxides[15,16] shows n-type behavior, which are typically used as electron selective interfaces over the transparent cathode. Zhou et al.[17] reported surface modification of conductive electrodes using an ultrathin layer of amine based polymers which served as electron selective layers for inverted polymer solar cells. Recently several papers[18–22] have shown enhancement in device performance using polymer surface modifier on electron selective metal oxide layers. However, the reason behind efficiency enhancement is still not clear and they also have not addressed the stability of the polymer solar cells with different interfacial layers.

Lower lifetime in organic solar cells could be attributed to degradation of several layers of the device which includes the active layer, electron and hole blocking layers, and electrodes. Oxygen adsorption and diffusion within the polymer−fullerene layer, in the case of the polythiophenes such as P3HT, leads to p-type doping, which induces limited mobility and poor charge transport because of the increase in trapped states. These trapped states are also present in the oxygen-induced doping of fullerenes such as Phenyl-C_{61}-butyric acid methyl ester ($PC_{61}BM$), where an oxygenated $PC_{61}BM$ molecule shows decreased LUMO energy levels in comparison to pristine $PC_{61}BM$ molecules.[23] These doped molecules within the $PC_{61}BM$ domains of the active layer establish additional trapped states, inhibiting free electron movement thus also leading to decreased mobility and poor charge transport. To overcome degradation of active layer morphology, we can tailor control and utilize novel polymers with higher HOMO levels and use of cross-linkers. Oxygen-induced degradation can occur in the metal oxide buffer layer as well because of polymers' relatively high gas permeability, which allows for atmospheric oxygen to diffuse through seemingly solid layers within the device.[7,24] Oxygen adsorption and photoinduced doping in the metal oxide buffer layers[25] such as zinc oxide, can also lead to poor device performance because of an increase in series resistance of the device. Oxygen adsorption in metal oxides also leads to low mobility, poor charge transport, and an increased amount of trapped states; all of which adversely affects device performance by increasing the probability of recombination within the device because of an introduction of defects and impurities.[25,26] With an increased recombination rate, the amount of free electrons and holes found at their respective electrodes decreases, lowering the power output of the device. Hence, passivation or enhancing the chemical resistance of metal oxide layers is crucial to attain higher lifetime in inverted polymer solar cells.

This work focuses on increasing the stability of organic photovoltaic devices and studying the effects of surface passivation on the hole blocking layer in an inverted structure device. Surface modification using thin cationic polymer layer reduced the reactivity of the metal oxide with adsorbed oxygen from the ambient atmosphere. This surface passivation prevents recombination and poor charge transport due to the reduction of trapped states formed at the polymer−metal oxide interface. Organic solar cells fabricated with such modified electron selective interface exhibited enhanced lifetime and showed minimal degradation over 180 days when stored in atmospheric conditions without any encapsulation. This work provides an economical approach to significantly enhance the stability of organic solar cells when exposed to ambient conditions without need for encapsulation.

■ EXPERIMENTAL SECTION

Zinc oxide (ZnO) sol−gel was synthesized according to the reported procedures.[27,28] The procedure involved stirring a solution overnight comprised of zinc acetate dihydrate (1 g) dissolved in 2-methoxyethanol (10 mL) with ethanolamine (0.28 g) as a stabilizer. Aluminum-doped zinc oxide (AZO) sol−gel was synthesized by stirring a solution of zinc acetate dihydrate (217 mg) in ethanol (10 mL) for 8 h at 80 °C as reported elsewhere.[29] The resultant solution after cooling was filtered by a 0.45 μm PTFE filter prior to storage. Both AZO and ZnO sol−gel solutions were filtered by a 200 nm PVDF filter before spin coating. Polyethylenimine, 80% ethoxylated (PEIE) solution in water was purchased from Sigma-Aldrich. The

solution was diluted using 2-methoxyethanol as a solvent to a final ratio of 0.1 wt % and stirred by a magnetic stir bar overnight.

The active layer solution involved poly(3-hexylthiophene) (P3HT) purchased from Rieke Metals; the molecular weight of P3HT was 50 000−70 000 determined by GPC from the manufacturer. Phenyl-C61-butyric acid methyl ester ($PC_{60}BM$) was purchased from Nano-C. The blend solution preparation and deposition was done according to our previous report.[30] Nitrobenzene (Sigma-Aldrich) was added (4% volume) to the blend solution 30 min prior to spin-casting the films.

Tin-doped indium oxide (ITO)-coated glass substrates, 1 cm × 1 cm × 1 mm (15 ohms/□, ITO thickness of 125 nm) were cleaned sequentially in 20 min sessions of ultrasonication in a solution of sodium dodecyl sulfate in deionized (DI) water, followed by DI water, acetone and isopropanol. The substrates were subsequently treated with oxygen plasma cleaning for 25 min to ash any leftover organic residue prior to spin coating. For the hole blocking layer, either ZnO sol−gel, AZO sol−gel, or PEIE was spin coated on the surface at 4500 rpm for 60 s, 3000 rpm for 40 s or 5000 rpm for 60 s respectively, with annealing parameters at 300 °C for 30 min for ZnO, 155 °C for 10 min for AZO or 120 °C for 10 min for PEIE. The thickness of PEIE is about 10 nm. Samples were then transferred to a nitrogen-filled glovebox before coating the active layer. The $P3HT:PC_{61}BM$ solution was coated at 600 rpm for 40 s, this resulted in a thickness of ∼180 nm. $P3HT:PC_{61}BM$ casted films were subjected to annealing at 150 °C for 10 min on a hot plate which were then transferred to a thermal evaporator for the deposition of the electron blocking layer molybdenum trioxide (MoO_3) and silver (Ag) electrode at corresponding thicknesses of ∼7 and 80 nm, respectively, at a base chamber pressure of 1×10^{-6} mbar. The active area used for the cells were 0.16 cm^2 measured by the overlap of anode and cathode.

A xenon (Xe) arc lamp with an air mass (AM) 1.5 filter was used as a solar simulator. A NREL-calibrated reference photodetector was used to calibrate the distance from the lamp to the sample to obtain an illumination intensity of 100 mW/cm^2. Devices were stored in the dark under ambient conditions (yemperature ∼25 °C and relative humidity ∼20%). Devices were periodically tested with above-mentioned AM 1.5 calibration before testing. Topography and surface potential images of the films were taken using an Agilent 5500 atomic force microscope. A Pt/Cr Silicon tip (Budget Sensors, Tap 300 EG) having resonant frequency ∼290 kHz and force constant of 40 N m^{-1} was used for these measurements. Both topography and surface potential images were taken simultaneously in single pass mode using two lock-in amplifiers. The first mechanical resonance frequency of tip was fed to the first lock-in amplifier (LIA 1) and an electrical bias (4 kHz, DC offset = −0.5 V) was fed to the conductive tip using the second lock-in amplifier (LIA 2). The Y-component of LIA 1 was fed as the input for LIA 2 and a servo was used to nullify the electrostatic amplitude induced due to the AC bias given by LIA 2. The same tip was used for all films and entire imaging was done in net attractive mode. The acquired images were then processed and analyzed using Gwyddion.

Photocharge extraction by linearly increasing voltage (CELIV) measurements were taken on fresh and aged ZnO or ZnO/PEIE devices using a nanosecond dye laser coupled with a nitrogen laser for excitation (OL-401 OBB Corp.). The voltage ramp and delay time were determined using a function generator (Rigol DG1022). The Photo-CELIV signals were recorded using Agilent MSO7034B oscilloscope. The synchronization between laser, function generator and oscilloscope was achieved through a custom written LabVIEW program. The delay times were varied from 250 ns to 100 μs using the LabVIEW program. A ramp voltage of 4 V in 12.5 μs was used for all devices. The devices were kept in open circuit conditions to ensure minimal charge extraction or injection. The charge carrier mobility were evaluated using as per reported procedure.[31] The point where the extracted current reaches the maximum was used with the immediate voltage from the applied voltage ramp, along with the active layer thickness, to calculate for the instantaneous electric field.
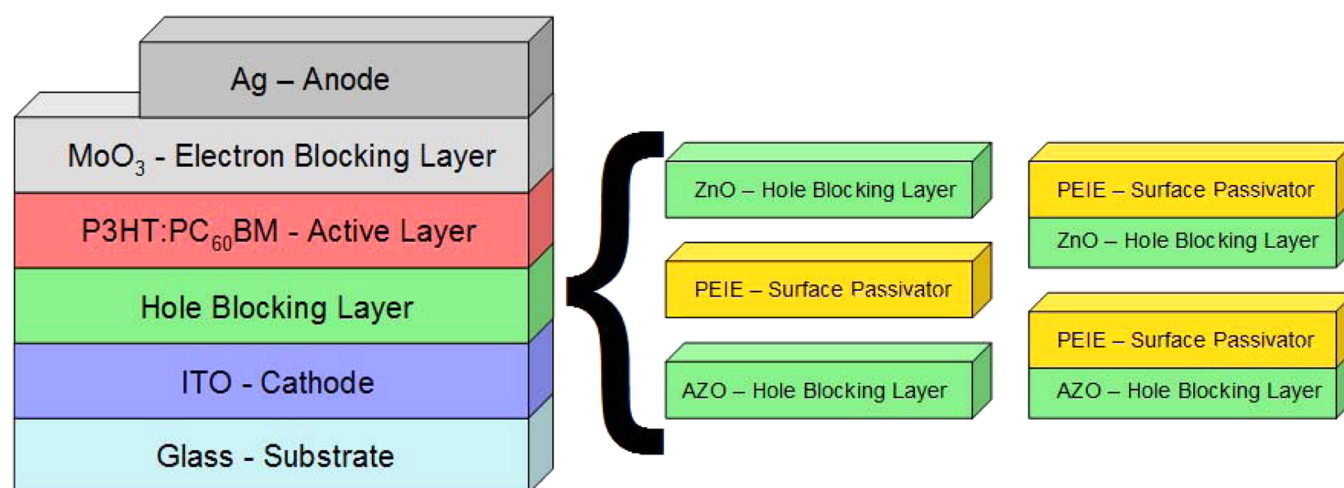
Figure 1. Solar cell device using an inverted structure.

Table 1. Device Characteristics in Terms of Open Circuit Voltage (V_{oc}), Short Circuit Current Density (J_{sc}), Fill Factor (FF), Efficiency (η), and Shunt (R_{sh}) and Series (R_s) Resistances for Fresh and 6 Month Aged Devices

	V_{oc} (V)		J_{sc} (mA/cm^2)		FF (%)		η (%)			R_{sh} (kΩ)		R_s (Ω)	
	fresh	aged	fresh	aged	fresh	aged	fresh	aged	η_{aged}/η_{fresh} ratio (%)	fresh	aged	fresh	aged
ZnO	0.60	0.61	11.09	7.88	0.60	0.47	4.01	2.28	56.95	9.3	3.0	1.57	22.40
ZnO/PEIE	0.62	0.63	10.61	9.09	0.62	0.62	4.07	3.56	87.45	3082	1990	2.17	5.55
PEIE	0.63	0.39	10.30	5.60	0.66	0.38	4.28	0.82	19.22	47	1.7	3.03	39.62
AZO/PEIE	0.62	0.64	9.77	7.29	0.67	0.65	4.05	3.04	74.94	816	416	2.69	5.38
AZO	0.61	0.62	10.83	7.43	0.65	0.54	4.32	2.50	57.96	7.1	5.4	1.69	8.71

■ RESULTS AND DISCUSSION

Figure 1 represents the fabricated inverted structure solar cell configuration. Device performance of P3HT:PC$_{61}$BM solar cells with different electron-selective interfaces was measured under illuminated conditions to observe the differences in the device degradation and determine the changes that occur at the hole blocking layer−active layer interface with and without the modification. Current density−voltage measurements were taken periodically as a time-varying degradation study. The time frame of this study was 178 days (∼6 months) from the initial fabrication date, with cells stored in atmospheric conditions for the entirety of the study. The terms "fresh" and "aged" will refer to the initial fabrication date and ∼6 months of aging respectively for the remainder of this paper, unless otherwise stated. Individual cells were recharacterized once per day for the first week, then once every week or every other week for the remainder of the study; this included measurements in both illuminated and dark conditions. The device results shown here represent average of at least 3−6 devices. The number of devices for each condition was identified by cells that showed similar efficiencies (standard deviation ±0.2%). The current−voltage measurements are shown in Figure S1, with results tabulated in Table 1.

Figure S1 shows the illuminated current density−voltage characterization, the photovoltaic parameters extracted from this measurement included V_{oc}, J_{sc}, FF, and η. Figure 2 shows the individual parameters of V_{oc}, J_{sc}, FF, and η as a function of time, which better represents the individual changes in each parameter as time progresses. The series (R_s) and shunt (R_{sh}) resistances of devices before and after aging were calculated using the dark current density−voltage measurements, which are shown in Figure 3. During the initial fabrication, each device

showed similar performance in terms of efficiency. Minor differences can be seen in the short circuit current density for ZnO and AZO samples compared to their PEIE-coated counterparts. The PEIE bilayer devices show a lower current density than hole blocking layers without the secondary coating. This is due to the additional insulating thin film increasing the series resistance within the device. The initial fill factors for devices using a hole blocking layer coated with PEIE are also larger, 0.62−0.67 compared to 0.6−0.65. This increase in fill factor can be due to a lower recombination probability from the lower (closer to vacuum) Fermi level. After aging, it can clearly be seen that a standalone layer of PEIE as a hole blocking layer is not as effective as the other metal oxide layers, as the degradation decreased device performance from 4.28 to 0.82%, 19% of its original efficiency. A relatively large decrease in the shunt resistance and increase in the series resistance, in comparison to other devices, shows a much higher internal leakage current and poorer charge transport for the PEIE device. It is noted that the PEIE-modified ZnO and AZO devices showed 87% and 74% of their original efficiency respectively, whereas unmodified ZnO and AZO devices only showed 56% and 57% of their original efficiencies. This also correlates to the larger Rsh and lower Rs observed over time for modified ZnO and AZO samples, which can be attributed to the reduced internal leakage currents and higher charge transport for longer device lifetime.

The V_{oc} of the PEIE-only devices quickly falls to below 0.4 V at only 50 days of ambient atmospheric exposure, while the others remain very stable. The Jsc for each device are shown to decrease steadily. This suggests that the active layer degradation is the major cause for the decrease in J_{sc} across all devices, with individual changes in Jsc being dependent on the metal oxide film, or lack thereof in the case of only surface passivation on
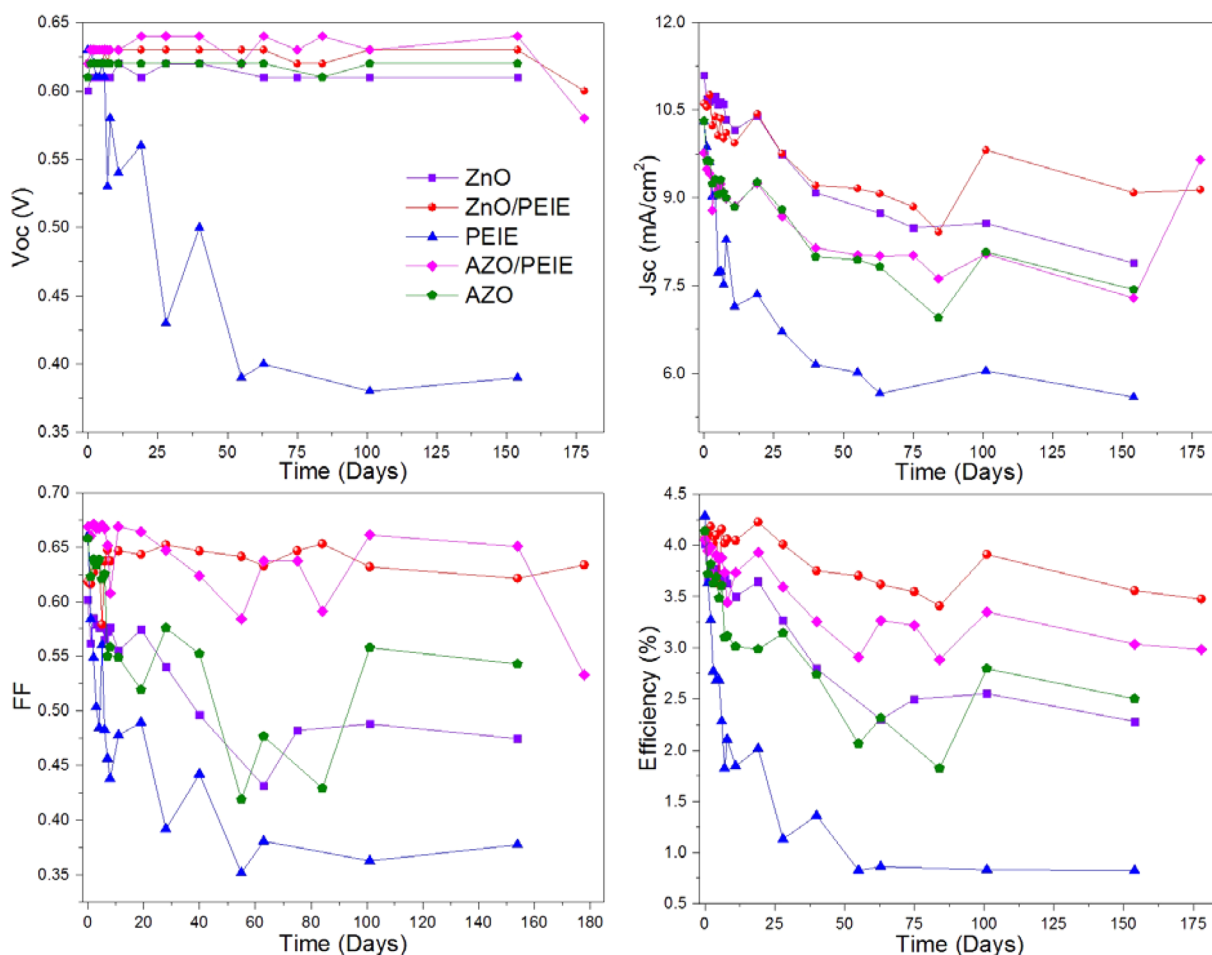
Figure 2. Current−voltage parameter breakdown of V_{oc}, J_{sc}, FF, and efficiency vs time in days.
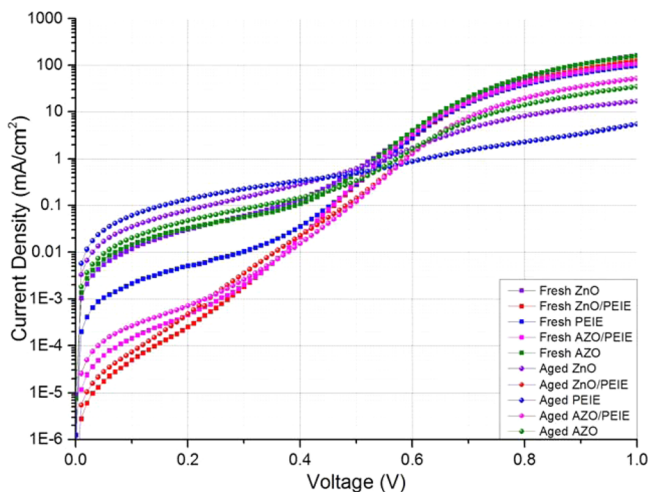

Figure 3. Dark current density−voltage characteristics for fresh and 6 month aged samples.

ITO by PEIE. The primary source of the differences in device efficiency is from the fill factor. The ZnO/PEIE and AZO/PEIE cells show a relatively stable fill factor, ∼0.62 over the course of the study, while the ZnO and AZO devices' fill factors decrease to ∼0.45 at 60 days of ambient exposure. Minor fluctuations in this data can be attributed to the mechanical degradation of the silver electrodes due to subsequent characterizations. Devices with a ZnO buffer layer showed higher current densities than

the AZO samples, which could be due to an enhanced interfacial area caused by the nanoridge formation in ZnO.[32] Band energy alignment differences between ZnO and AZO were also considered as a possibility of the difference in current densities. From the illuminated current density−voltage curves, it can be clearly seen that modifying ZnO and AZO by a thin film of PEIE provides a much longer degradation cycle than the bare buffer layers. The observed short circuit current density and their trends were consistent with the trends observed in the EQE spectra for each device (Figure S2 in the Supporting Information).

Figure 3 shows the dark current−voltage measurements for both fresh and aged samples. The ZnO/PEIE and AZO/PEIE devices have relatively lower leakage currents at low bias as compared to the devices without the PEIE modification. After half a year of ambient exposure, the bilayer devices maintained smaller current densities at low bias than fresh samples with standalone buffer layers. However, the devices using other hole blocking layers such as ZnO, AZO, or PEIE only exhibited higher current densities than fresh samples at low bias. This follows the shunt resistance value trend in Table 1. The PEIE device experienced the largest increase in leakage current at a low bias of 10 mV and also the biggest decrease in saturation current at a higher bias (of 1 V). Electronically, the degradation dynamics shift the devices' current−voltage pattern to behave more as a resistor than a diode in dark conditions. This shift can be better seen in the Figure S3 in the Supporting Information, where images of individual cells' dark curves are

shown with arrows marking the change in current density as time progresses. These changes can be due to oxygen-induced trapped states, which increase the probability of trap-assisted recombination and decrease the charge transport, shown in low and high voltage biases, respectively.

Table 2 shows Kelvin probe Fermi level measurements on fresh and aged hole blocking layers. The proposed hypothesis is

Table 2. Kelvin Probe Measurement Results Showing Fermi Levels (away from vacuum) of Fresh and 4 Day Aged Hole Blocking Layers

	Fermi level (eV)	
	fresh	aged (4 days)
ZnO	−4.49	−4.56
ZnO/PEIE	−4.18	−4.13
PEIE	−4.15	−4.19
AZO/PEIE	−4.23	−4.17
AZO	−4.15	−4.40

that modifying the metal oxide layer with PEIE leads to passivation of the oxide surface, preventing further oxidation. This passivated surface lowers the probability of trap-assisted recombination at the metal oxide-polymer interface. This can be seen from the enhancement in the Fermi level stability over time as shown in Table 2, where ZnO, AZO, and PEIE show deeper Fermi levels away from vacuum, however ZnO/PEIE and AZO/PEIE show shallower Fermi levels, toward the vacuum level. Correlating these results to the dark current–

voltage characteristics shown in Figure 3, a Fermi level closer to that of vacuum would be further away from the valence band of P3HT, thus reducing the probability of recombination between the Fermi level of oxide and HOMO level of P3HT. This stability in the Fermi levels for the PEIE-coated ZnO and AZO films show a decreased reactivity with ambient oxygen compared to the ZnO- and AZO-only films. The changes in Femi levels were also observed by using Kelvin probe force microscopy (KPFM) measurements on the ZnO and ZnO/PEIE films as shown in Figure 4.

No significant change in surface morphology and roughness was observed in topographic images (Figure S4 in Supporting Information). Figure 4 represents the surface potential maps of freshly prepared and aged ZnO and ZnO/PEIE films, taken by KPFM measurements. KPFM measures the contact potential difference between the tip and the sample, denoted as the surface potential. Comparing the freshly prepared films, ZnO shows a lower surface potential than ZnO/PEIE, which correlates to the Kelvin probe measurements found earlier and in line with KPFM of ZnO and PEIE interface as shown in Figure S5 of Supporting Information. As oxidation occurred from ambient exposure, the ZnO sample showed a larger decrease in the average surface potential than the ZnO/PEIE sample. This also correlates to what was observed in Table 2, as the Fermi levels for ZnO/PEIE was closer to vacuum level, compared to the ZnO-only film.

Figure 5 shows a plot of distribution vs surface potential for the fresh and 7 days aged ZnO and ZnO/PEIE samples. No change in the surface potential distribution shape was observed
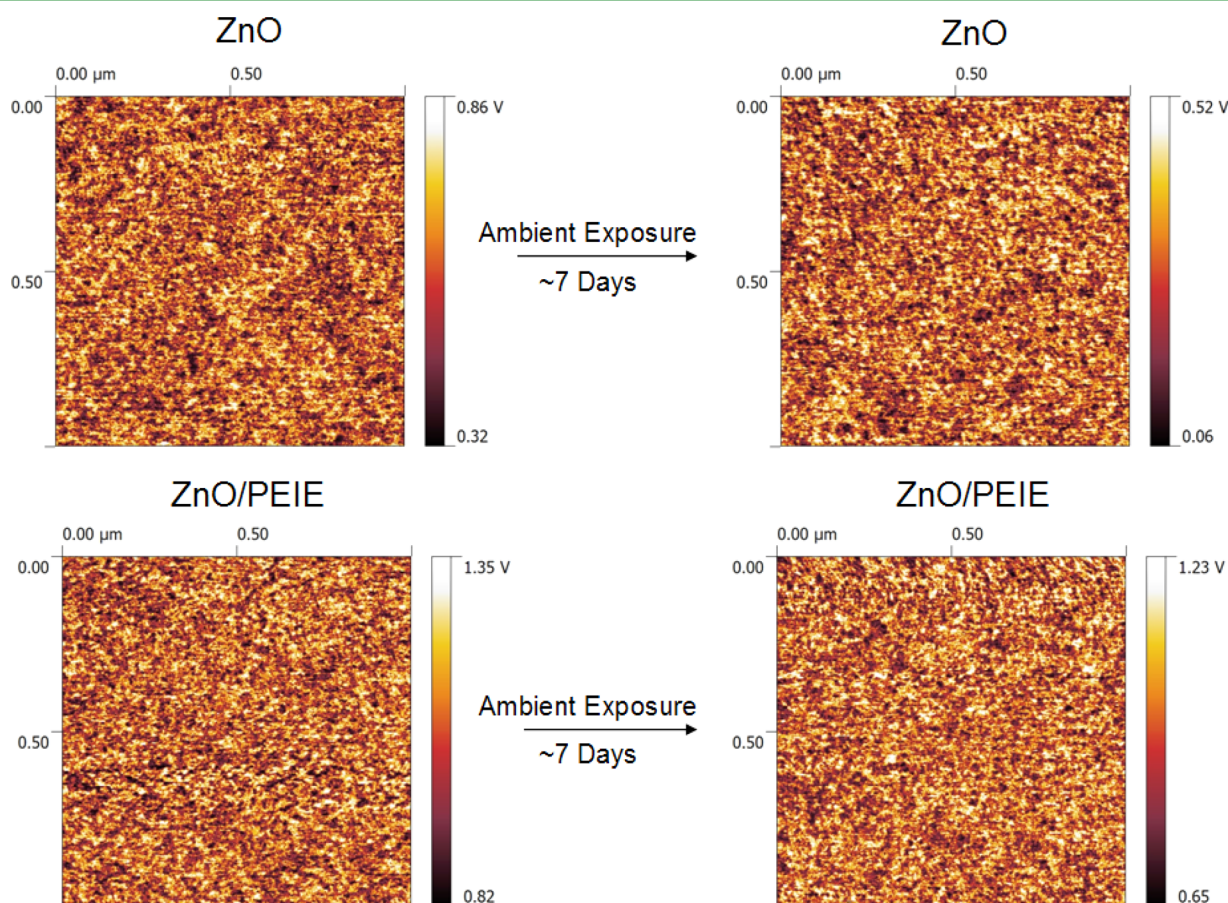

Figure 4. KPFM surface potential images of ZnO and ZnO/PEIE films without and with ambient exposure. Image sizes are 1 μm × 1 μm.
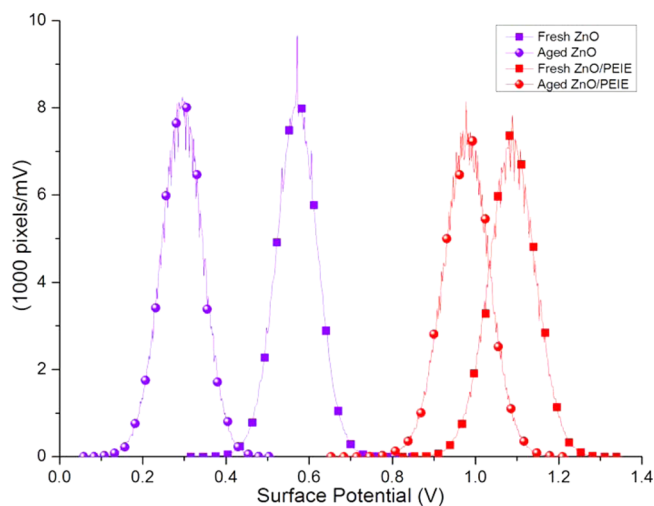
Figure 5. Distribution vs surface potential for the fresh and 7 days aged ZnO and ZnO/PEIE films.

for any sample, where the full width at half-maximum is comparable between different samples. As described earlier, the change in surface potential is much greater for the ZnO film compared to the ZnO/PEIE film. The reason for this difference in surface potential change can be attributed to the less oxygenated ZnO molecules in the ZnO/PEIE film because o the surface passivation by PEIE, which reduces the amount of trapped states from forming by oxygen doping.

Figure 6 shows the process of trap-assisted recombination at the hole blocking layer-active layer interface. Gas permeability
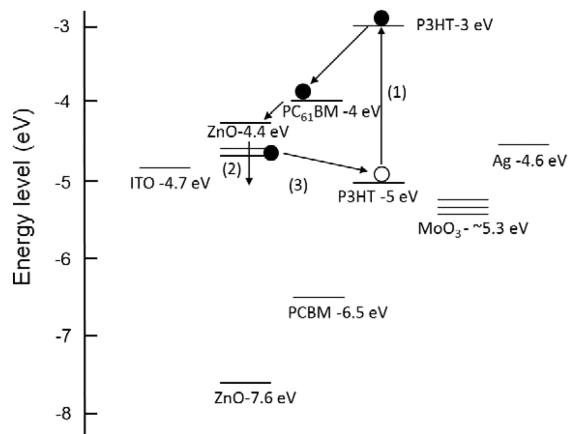

Figure 6. Graphical representation of oxygen-induced degradation and trap-assisted recombination at the ZnO-P3HT interface after aged. The values shown are in terms of electron volts (eV) away from the vacuum level. (1) Light absorption, (2) oxidation, and (3) trap-assisted recombination.

in the polymer active layer allows for oxygen to pass through, which may then embed onto the surface of the ZnO layer and diffuse further.[33] This induces a deeper average Fermi level as trapped states appear within the ZnO film, which then trap free electrons from moving to the ITO electrode. It was found that over time, the Fermi level of the ZnO and AZO films move away from the vacuum level, closer to the value of the adjacent P3HT valence band. From here, trapped electrons may easily recombine with the holes in the polymer, which increases the

internal leakage current within the device, thus reducing the power output of the device.

Figure 7 represents the device mobility vs the electric field at the maximum charge extraction point. From the analysis of
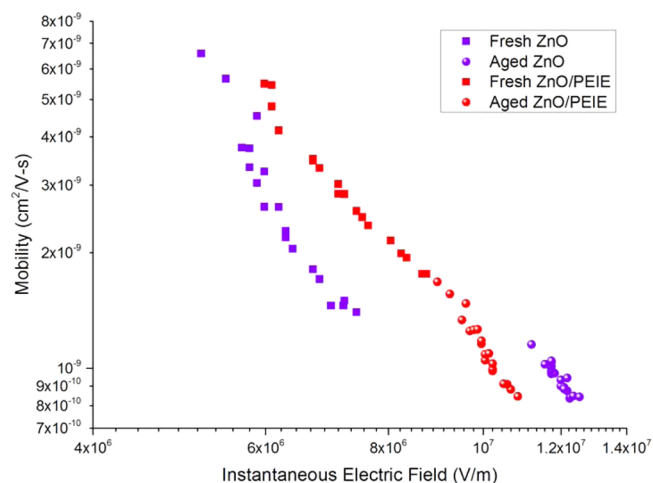

Figure 7. Mobility vs instantaneous electric field for the fresh and 6 months aged ZnO and ZnO/PEIE devices.

device degradation due to exposure to atmospheric conditions, the device mobility can decrease over time because of impurity doping. As the devices are aged, their carrier mobility decreases. A difference between the ZnO and ZnO/PEIE devices is that the required electric field for extracting maximum charge is lower initially for the ZnO device than that for the ZnO/PEIE device. This could be due to the thin dielectric PEIE coating, behaving as a tunneling interface, which would hinder electron extraction, hence requiring a slightly higher bias voltage to efficiently extract all the photogenerated carriers. However, as the devices are aged, the electric field at the maximum charge extraction point becomes lower for the ZnO/PEIE device than it is for the ZnO device. This shows that the ZnO/PEIE device is less affected by aging in atmospheric conditions as compared to that without the PEIE layer. The reduced degradation is attributed to the surface passivation from PEIE, which reduces the reactivity and inhibits doping of atmospheric oxygen at this interface. The reduced doping and impurity diffusion at this layer reduces the amount of trapped states forming, which in turn requires a lower electric field to extract the maximum possible amount of charge. The mobility for the aged ZnO/PEIE devices (3.33×10^{-3} cm^2 V^{-1} s^{-1}) also showed as a higher average than the aged ZnO devices (2.75×10^{-3} cm^2 V^{-1} s^{-1}). This difference in mobility for the aged devices is attributed to the reduced amount of trapped states within the bilayer buffer layer, which supports the dependence of device performance on the mobility of the hole blocking layer.

■ CONCLUSIONS

The stability of bulk heterojunction solar cells were investigated with bare and surface modified metal oxide layers as the hole blocking layer. Results showed enhanced lifetimes by 54 and 29% for devices with PEIE modified ZnO and AZO interfaces respectively compared to bare ZnO and AZO as an electron-selective interface. The enhancement in lifetime was attributed to the stable fill factors arising from the suppressed oxidation of metal oxide layers when passivated with PEIE. Bare metal oxide surfaces are prone to oxidation, which leads to an increase in

Fermi level and formation of trap states. These trap states, present at the interface between active layer and hole blocking layer, exhibit a higher recombination of photogenerated charges and also a suppressed charge transport in the buffer layer that led to a drastic reduction in short circuit current density and fill factor when the devices were stored in atmospheric conditions. Photo-CELIV measurements on fresh and aged devices showed that a higher electric field was required for devices with a bare ZnO surface with aging. Aged devices with a ZnO/PEIE interface required a lower electric field for maximum charge extraction than the aged ZnO device. This was correlated to the reduced amount of trapped states forming at the ZnO/PEIE/P3HT:PC$_{61}$BM interface. Solution-based modification can therefore act as a potential low-cost method to passivate interfacial layers to enhance the device lifetime in organic solar cells.

■ ASSOCIATED CONTENT

Ⓢ Supporting Information

Illuminated current−voltage characteristics and EQE vs wavelength in nm for fresh and aged P3HT:PCBM devices; Individual device dark current−voltage curves for up to 154 days of degradation in atmospheric conditions; AFM Topography images and surface potential image. The Supporting Information is available free of charge on the ACS Publications website at DOI: 10.1021/acsami.5b04687.

■ AUTHOR INFORMATION

Corresponding Author
*E-mail: qiquan.qiao@sdstate.edu.

Author Contributions
†S.V. and E.N. contributed equally to this work

Notes
The authors declare no competing financial interest.

■ ACKNOWLEDGMENTS

■ REFERENCES

(1) Krebs, F. C. Fabrication and Processing of Polymer Solar Cells: A Review of Printing and Coating Techniques. *Sol. Energy Mater. Sol. Cells* **2009**, *93*, 394−412.

(2) Li, G.; Zhu, R.; Yang, Y. Polymer Solar Cells. *Nat. Photonics* **2012**, *6*, 153−161.

(3) Venkatesan, S.; Chen, Q.; Ngo, E. C.; Adhikari, N.; Nelson, K.; Dubey, A.; Sun, J.; Bommisetty, V.; Zhang, C.; Galipeau, D.; Qiao, Q. Polymer Solar Cells Processed Using Anisole as a Relatively Nontoxic Solvent. *Energy Technol.* **2014**, *2*, 269−274.

(4) Aernouts, T.; Aleksandrov, T.; Girotto, C.; Genoe, J.; Poortmans, J. Polymer based Organic Solar Cells using Ink-jet Printed Active Layers. *Appl. Phys. Lett.* **2008**, *92*, 033306.

(5) Ngo, E.; Venkatesan, S.; Qiao, Q. Polymer Photovoltaics With Top Metal Electrode Deposited by Solution-Processing. *IEEE Trans. Electron Devices* **2014**, *61*, 2957−2962.

(6) Ngo, E.; Venkatesan, S.; Galipeau, D.; Qiao, Q. Polymer Photovoltaic Performance and Degradation on Spray and Spin Coated Electron Transport Layer and Active Layer. *IEEE Trans. Electron Devices* **2013**, *60*, 2372−2378.

(7) Norrman, K.; Madsen, M. V.; Gevorgyan, S. A.; Krebs, F. C. Degradation Patterns in Water and Oxygen of an Inverted Polymer Solar Cell. *J. Am. Chem. Soc.* **2010**, *132*, 16883−16892.

(8) Jørgensen, M.; Norrman, K.; Krebs, F. C. Stability/Degradation of Polymer Solar Cells. *Sol. Energy Mater. Sol. Cells* **2008**, *92*, 686−714.

(9) Yun, J.-M.; Yeo, J.-S.; Kim, J.; Jeong, H.-G.; Kim, D.-Y.; Noh, Y.-J.; Kim, S.-S.; Ku, B.-C.; Na, S.-I. Solution-Processable Reduced Graphene Oxide as a Novel Alternative to PEDOT:PSS Hole Transport Layers for Highly Efficient and Stable Polymer Solar Cells. *Adv. Mater.* **2011**, *23*, 4923−4928.

(10) Sun, Y.; Takacs, C. J.; Cowan, S. R.; Seo, J. H.; Gong, X.; Roy, A.; Heeger, A. J. Efficient, Air-Stable Bulk Heterojunction Polymer Solar Cells Using MoOx as the Anode Interfacial Layer. *Adv. Mater.* **2011**, *23*, 2226−2230.

(11) He, Z.; Zhong, C.; Su, S.; Xu, M.; Wu, H.; Cao, Y. Enhanced Power-conversion Efficiency in Polymer Solar Cells using an Inverted Device Structure. *Nat. Photonics* **2012**, *6*, 591−595.

(12) Guo, X.; Zhou, N.; Lou, S. J.; Smith, J.; Tice, D. B.; Hennek, J. W.; Ortiz, R. P.; Navarrete, J. T. L.; Li, S.; Strzalka, J.; Chen, L. X.; Chang, R. P. H.; Facchetti, A.; Marks, T. J. Polymer Solar Cells with Enhanced Fill Factors. *Nat. Photonics* **2013**, *7*, 825−833.

(13) Hau, S. K.; Yip, H.-L.; Baek, N. S.; Zou, J.; O'Malley, K.; Jen, A. K.-Y. Air-stable Inverted Flexible Polymer Solar Cells using Zinc Oxide Nanoparticles as an Electron Selective Layer. *Appl. Phys. Lett.* **2008**, *92*, 253301.

(14) Waldauf, C.; Morana, M.; Denk, P.; Schilinsky, P.; Coakley, K.; Choulis, S. A.; Brabec, C. J. Highly Efficient Inverted Organic Photovoltaics using Solution based Titanium Oxide as Electron Selective Contact. *Appl. Phys. Lett.* **2006**, *89*, 233517.

(15) Chen, S.; Manders, J. R.; Tsang, S.-W.; So, F. Metal Oxides for Interface Engineering in Polymer Solar Cells. *J. Mater. Chem.* **2012**, *22*, 24202−24212.

(16) Siddiki, M. K.; Venkatesan, S.; Qiao, Q. Nb2O5 as a New Electron Transport Layer for Double Junction Polymer Solar Cells. *Phys. Chem. Chem. Phys.* **2012**, *14*, 4682−4686.

(17) Zhou, Y.; Fuentes-Hernandez, C.; Shim, J.; Meyer, J.; Giordano, A. J.; Li, H.; Winget, P.; Papadopoulos, T.; Cheun, H.; Kim, J.; Fenoll, M.; Dindar, A.; Haske, W.; Najafabadi, E.; Khan, T. M.; Sojoudi, H.; Barlow, S.; Graham, S.; Brédas, J.-L.; Marder, S. R.; Kahn, A.; Kippelen, B. A Universal Method to Produce Low−Work Function Electrodes for Organic Electronics. *Science* **2012**, *336*, 327−332.

(18) Kyaw, A. K. K.; Wang, D. H.; Gupta, V.; Zhang, J.; Chand, S.; Bazan, G. C.; Heeger, A. J. Efficient Solution-Processed Small-Molecule Solar Cells with Inverted Structure. *Adv. Mater.* **2013**, *25*, 2397−2402.

(19) Mitul, A. F.; Mohammad, L.; Venkatesan, S.; Adhikari, N.; Sigdel, S.; Wang, Q.; Dubey, A.; Khatiwada, D.; Qiao, Q. Low Temperature Efficient Interconnecting Layer for Tandem Polymer Solar Cells. *Nano Energy* **2015**, *11*, 56−63.

(20) Shim, J. W.; Fuentes-Hernandez, C.; Zhou, Y.; Dindar, A.; Khan, T. M.; Giordano, A. J.; Cheun, H.; Yun, M.; Marder, S. R.; Kippelen, B. Inverted Tandem Polymer Solar Cells with Polyethylenimine-Modified MoOX/Al2O3:ZnO Nanolaminate as the Charge Recombination Layers. *Adv. Energy Mater.* **2014**, *4*, 1400048.

(21) Yuan, K.; Chen, L.; Chen, Y. Versatile Electron-Collecting Interfacial Layer by in Situ Growth of Silver Nanoparticles in Nonconjugated Polyelectrolyte Aqueous Solution for Polymer Solar Cells. *J. Phys. Chem. B* **2014**, *118*, 11563−11572.

(22) Li, P.; Cai, L.; Wang, G.; Zhou, D. C.; Xiang, J.; Zhang, Y. J.; Ding, B. F.; Alameh, K.; Song, Q. L. PEIE Capped ZnO as Cathode Buffer Layer with Enhanced Charge Transfer Ability for High Efficiency Polymer Solar Cells. *Synth. Met.* **2015**, *203*, 243−248.

(23) Reese, M. O.; Nardes, A. M.; Rupert, B. L.; Larsen, R. E.; Olson, D. C.; Lloyd, M. T.; Shaheen, S. E.; Ginley, D. S.; Rumbles, G.; Kopidakis, N. Photoinduced Degradation of Polymer and Polymer−Fullerene Active Layers: Experiment and Theory. *Adv. Funct. Mater.* **2010**, *20*, 3476−3483.

(24) Andersen, M.; Carlé, J. E.; Cruys-Bagger, N.; Lilliedal, M. R.; Hammond, M. A.; Winther-Jensen, B.; Krebs, F. C. Transparent Anodes for Polymer Photovoltaics: Oxygen Permeability of PEDOT. *Sol. Energy Mater. Sol. Cells* **2007**, *91*, 539−543.

(25) Cowan, S. R.; Schulz, P.; Giordano, A. J.; Garcia, A.; MacLeod, B. A.; Marder, S. R.; Kahn, A.; Ginley, D. S.; Ratcliff, E. L.; Olson, D. C. Chemically Controlled Reversible and Irreversible Extraction Barriers Via Stable Interface Modification of Zinc Oxide Electron Collection Layer in Polycarbazole-based Organic Solar Cells. *Adv. Funct. Mater.* **2014**, *24*, 4671−4680.

(26) MacLeod, B. A.; Tremolet de Villers, B. J.; Schulz, P.; Ndione, P. F.; Kim, H.; Giordano, A. J.; Zhu, K.; Marder, S. R.; Graham, S.; Berry, J. J.; Kahn, A.; Olson, D. C. Stability of Inverted Organic Solar Cells with ZnO Contact Layers Deposited from Precursor Solutions. *Energy Environ. Sci.* **2015**, *8*, 592−601.

(27) Venkatesan, S.; Adhikari, N.; Chen, J.; Ngo, E. C.; Dubey, A.; Galipeau, D. W.; Qiao, Q. Interplay of Nanoscale Domain Purity and Size on Charge Transport and Recombination Dynamics in Polymer Solar Cells. *Nanoscale* **2014**, *6*, 1011−1019.

(28) Sun, Y.; Seo, J. H.; Takacs, C. J.; Seifter, J.; Heeger, A. J. Inverted Polymer Solar Cells Integrated with a Low-Temperature-Annealed Sol-Gel-Derived ZnO Film as an Electron Transport Layer. *Adv. Mater.* **2011**, *23*, 1679−1683.

(29) Stubhan, T.; Litzov, I.; Li, N.; Salinas, M.; Steidl, M.; Sauer, G.; Forberich, K.; Matt, G. J.; Halik, M.; Brabec, C. J. Overcoming Interface Losses in Organic Solar Cells by Applying Low Temperature, Solution Processed Aluminum-doped Zinc Oxide Electron Extraction Layers. *J. Mater. Chem. A* **2013**, *1*, 6004−6009.

(30) Venkatesan, S.; Chen, J.; Ngo, E. C.; Dubey, A.; Khatiwada, D.; Zhang, C.; Qiao, Q. Critical Role of Domain Crystallinity, Domain Purity and Domain Interface Sharpness for Reduced Bimolecular Recombination in Polymer Solar Cells. *Nano Energy* **2015**, *12*, 457−467.

(31) Venkatesan, S.; Ngo, E. C.; Chen, Q.; Dubey, A.; Mohammad, L.; Adhikari, N.; Mitul, A. F.; Qiao, Q. Benzothiadiazole-based Polymer for Single and Double Junction Solar Cells with High Open Circuit Voltage. *Nanoscale* **2014**, *6*, 7093−7100.

(32) Sekine, N.; Chou, C.-H.; Kwan, W. L.; Yang, Y. ZnO Nano-ridge Structure and its Application in Inverted Polymer Solar Cell. *Org. Electron.* **2009**, *10*, 1473−1477.

(33) Saravanan, S.; Ramamurthy, P. C.; Madras, G. Effects of Temperature and Clay Content on Water Absorption Characteristics of Modified MMT Clay/cyclic Olefin Copolymer Nanocomposite Films: Permeability, Dynamic Mechanical Properties and the Encapsulated Organic Device Performance. *Composites, Part B* **2015**, *73*, 1−9.